

Dust vortex flow analysis in weakly magnetized plasma

Prince Kumar* Devendra Sharma†

*Institute for Plasma Research, HBNI, Bhat, Gandhinagar - 382 428, Gujarat, India, and
Homi Bhabha National Institute, Mumbai, Maharashtra-400 094, India*

(Dated: June 4, 2020)

Analysis of driven dust vortex flow is presented in a weakly magnetized plasma. The 2D hydrodynamic model is applied to the confined dust cloud in a non-uniform magnetic field in order to recover the dust vortex flow driven in a conservative force field setup, in absence of any non-conservative fields or dust charge variation. Although the time independent electric and magnetic fields included in the analysis provide conservative forcing mechanisms, when the a drift based mechanism, recently observed in a dusty plasma experiment by [M. Puttscher and A. Melzer, Physics of Plasmas, 21,123704(2014)] is considered, the dust vortex flow solutions are shown to be recovered. We have examined the case where purely ambipolar electric field, generated by polarization produced by electron $\mathbf{E} \times \mathbf{B}$ drift, drives the dust flow. A sheared $\mathbf{E} \times \mathbf{B}$ drift flow is facilitated by the magnetic field gradient, driving the vortex flow in the absence of ion drag. The analytical stream-function solutions have been analyzed with varying magnetic field strength, its gradient and kinematic viscosity of the dust fluid. The effect of \mathbf{B} field gradient is analyzed which contrasts that of \mathbf{E} field gradient present in the plasma sheath.

PACS numbers: 36.40.Gk, 52.25.Os, 52.50.Jm

I. INTRODUCTION

Vortex flow in a charged fluid are highly relevant to generation of magnetic fields in nature and equilibrium configurations of magnetic confinement plasma experiments [1]. Quasi neutral electron-ion plasmas with highly charged dust particles present as third species [2], or a dusty plasma, provides a setup where vortex flow of the charged dust fluid is often present [3] and can be studied at very accessible spatio-temporal scale. The dust vortex flow in plasmas is modeled using the macroscopic 2D hydrodynamic formulation in magnetized plasma. The effects of an ambient magnetic field are expected to be moderate on the dust as long as the magnetic field is not strong enough to magnetize the dust particles. Recent experimental studies have however shown that in a weakly magnetized plasma where only electrons are magnetized, dust motion can have finite effects of the magnetic field via magnetization of electrons [4–7]. This paper presents a hydrodynamic formulation for the dust vortex flow accounting for effects of weak magnetization as observed and quantified in these recent experiments. With the availability of advanced magnetized dusty plasma experiments like MDPX [8, 9] the steady of collective dust dynamics, described here in weak to strongly magnetized plasma regime, may be possible with greater flexibility.

The existing dusty plasma studies show that the dust species in a plasma is subjected to various forces. The effects of forces on dust due to ion drag [10, 11], neutral drag and electrostatic forces, has been extensively studied both experimentally and theoretically in literature. Dust Vortex flow structures which are driven by non-conservative force fields, like ion drag force [12], neutral flow [13–15] have been observed in experiments. Dust Vortex flow have also been observed un-

der external forces [1, 16–19]. Recently, rotating dust structures have also been observed in weakly magnetized plasmas [4–7] where dust dynamics is again interpreted as governed by the non-conservative forces like, ion drag and neutrals flow.

In laboratory experiment, dynamics of both para magnetic and diamagnetic (Melamine-formaldehyde or MF) particles was investigated in the presence of gradient in magnetic field by Puttscher and Melzer [20], finding that only para-magnetic particles responded to magnetic field gradient. An interesting dynamics of diamagnetic particles was however also reported by Puttscher and Melzer [21] which is governed by an ambipolar electric field generated due to magnetized drifting electrons. Since the charged dust particles respond directly to an electrostatic field, their motion is governed by a conservative field which in usual cases does not produce a vortex flow, unlike a nonuniform drag or frictional force [10, 11]. In this work we analyze the dust flow in a weakly magnetized setup with a similar ambipolar forcing field and recover the dust vortex flow when the magnetic field has finite gradient.

Melzer and Puttscher [22] presented a force balance mechanism that can explain the motion of dust particles in the presence of weak homogeneous magnetic field. Since only electrons were magnetized and drifted in $\mathbf{E} \times \mathbf{B}$ direction, they produced an ambipolar electric field that acted both on the ions and the dust particles. They observed that although at low gas pressure, motion of dust particle was driven by the ion drag which acted flow along $\mathbf{E} \times \mathbf{B}$, at sufficiently high gas pressure the overall dust dynamics was governed purely by the ambipolar electric field and they moved against the $\mathbf{E} \times \mathbf{B}$ direction.

The $\mathbf{E} \times \mathbf{B}$ effect on dust particles observed by Melzer and Puttscher [22] arises because of a sheath electric field. Since this may be strongly sheared in the sheath region, it motivates the idea as to whether a sheared $\mathbf{E} \times \mathbf{B}$ drift can drive a vortex motion of a suspended dust fluid. Considering this, we study driven flow field of confined dust fluid which is suspended in the plasma sheath in the presence of a non-uniform weak magnetic field. Our analysis shows that the ambipolar elec-

* kumarprincephysics@gmail.com

† devendra@ipr.res.in

tric field can act as a source of finite vorticity in the dust flow dynamics. We derive and use the circulation of the ambipolar field generated by $\mathbf{E} \times \mathbf{B}$ drift of the electrons as a driver for vortex flow of the dust motion and study its behavior in presence of nonuniform magnetic field. The results show dependence of intensity of dust vortex motion on the strength of magnetic field and its gradient.

The paper is organized as follows. The 2D hydrodynamic model for confined dust fluid, in Cartesian geometry, with non-uniform magnetic field is introduced in sec.(II). In sec. (III) a boundary value problem constructed in Cartesian geometry for dust stream-function. In order to find analytic dust stream-function solutions, the boundary value problem is converted into an eigenvalue problem in which the dust stream-function and the driver are expressed in terms of suitable eigenfunctions. Dust stream-function solution is analyzed in sec. (IV) with variation in applied non-uniform magnetic field and kinematic viscosity μ of dust fluid. Dust vortex solutions for multipolar form of the ambipolar field are analyzed in sec.(V). The summary and conclusion of the result has been presented in sec.(VII).

II. THE DUST VORTEX MODEL IN A WEAKLY MAGNETIZED PLASMA

The setup of confined dust fluid considered here is motivated by the experiment by Puttscher and Melzer [21], who studied the behavior of dust particle motion in mutually perpendicular electric and magnetic field in the sheath region of an rf discharge. We consider a dust cloud modeled as a fluid suspended in plasma where both electrostatic and gravitational fields acting on it are mutually balanced. A nonuniform magnetic field is considered with a variation approximated as linear over a relatively small dimension of the dust confinement region as compared to scale lengths of the variation. In a Cartesian setup as described in Fig. 1, we accordingly use a magnetic field aligned with y axis with its variation along z axis, $\mathbf{B}(z) = B_0(1 + \alpha z)\hat{\mathbf{y}}$, produced locally, for example, by a section of a coil directed along x while coil axis directed along y -direction. A constant sheath electric field $\mathbf{E} = E_s\hat{\mathbf{z}}$ is considered present in the z -direction.

We study the 2-dimension dust fluid dynamics in a $x-z$ plane in a dust confinement domain ranging in the limits, $0 < x/L_x < 1$ and $0 < z/L_z < 1$, respectively; assuming symmetry along y . The basic hydrodynamics equations include the z and x components of the Navier-Stokes equation,

$$\frac{\partial U_z}{\partial t} + U_z \frac{\partial U_z}{\partial z} + U_x \frac{\partial U_z}{\partial x} = -\frac{1}{\rho} \frac{\partial P}{\partial z} - \frac{\partial V}{\partial z} + \mu \nabla^2 U_z + \frac{q_d}{m_d} E_a - \nu(U_z - W_z), \quad (1)$$

$$\frac{\partial U_x}{\partial t} + U_z \frac{\partial U_x}{\partial z} + U_x \frac{\partial U_x}{\partial x} = -\frac{1}{\rho} \frac{\partial P}{\partial x} - \frac{\partial V}{\partial x} + \mu \nabla^2 U_x + \frac{q_d}{m_d} E_a - \nu(U_x - W_x), \quad (2)$$

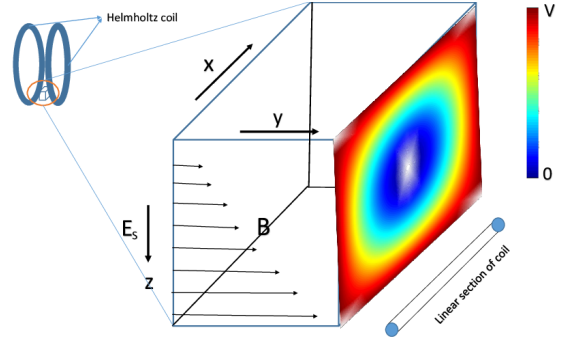


Figure 1: Schematic of the set up in Cartesian geometry with the contour plot showing the strength of effective confining potential $V(z,x)$ for the dust fluid.

respectively, and equation of continuity for the incompressible dust fluid, $\nabla \cdot \mathbf{U} = 0$, written as,

$$\frac{\partial U_z}{\partial z} + \frac{\partial U_x}{\partial x} = 0, \quad (3)$$

where V is the effective confining potential, q_d and m_d are the dust charge and mass, respectively, \mathbf{U} is the dust velocity and \mathbf{W} is the flow velocity of the neutral fluid. P and ρ are the pressure and mass density of the dust fluid, respectively, ν is coefficient of the friction with the neutral fluid acting on the dust and μ is its kinematic viscosity. The ion drag is ignored considering the limit of high pressure [21] where the dust dynamics is mainly governed by the ambipolar field \mathbf{E}_a due to electron fluid drifting past ions with the $E \times B$ drift perpendicular to the plane containing \mathbf{E} and \mathbf{B} .

We estimate \mathbf{E}_a from the current density \mathbf{j} of the drifting electrons. We begin by considering the electron momentum balance for time independent condition in presence of resistivity η ,

$$0 = \mathbf{E}_T + \mathbf{v}_e \times \mathbf{B} - \eta \mathbf{j}, \quad (4)$$

where $\mathbf{E}_T = \mathbf{E} + \mathbf{E}_a$ and

$$\mathbf{j} = n_e q_e \mathbf{v}_e, \quad (5)$$

where q_e is the elementary charge on electron and n_e is electron density. As mentioned above, $\mathbf{E} = E_s \hat{\mathbf{z}}$, and $\mathbf{B} = B \hat{\mathbf{y}}$ are externally applied fields. In the absence of resistivity $\eta \mathbf{j} = \mathbf{E}_a = 0$ and the lowest order expression for the force balance, containing terms directed purely along the z -axis, is recovered,

$$0 = \mathbf{E} + \mathbf{v}_e \times \mathbf{B}, \quad (6)$$

which yields the $E \times B$ velocity directed along $-\hat{\mathbf{x}}$,

$$\mathbf{v}_e = \frac{\mathbf{E} \times \mathbf{B}}{|\mathbf{B}|^2}. \quad (7)$$

When resistivity η is finite, i.e., electrons lose momentum via collisions while drifting along x , the frictional force $-\eta \mathbf{j}$ must

be balanced by a correction in the electric field (or in the effective drift) as required in the equilibrium state, such that the general force equilibrium (4) emerges. For the case $E_a \ll E$, when the lowest order equilibrium (6) can be subtracted from (4), the residual force balance, predominantly along x -axis, reads,

$$0 = \mathbf{E}_a - \eta \mathbf{j}. \quad (8)$$

Thus \mathbf{E}_a can be estimated if the lowest order $E \times B$ drift expression (7) is used to determine the current density \mathbf{j} given by (5) which is then substituted in Eq. (8), obtaining,

$$\mathbf{E}_a \approx \eta n_e q_e \frac{\mathbf{E} \times \mathbf{B}}{|\mathbf{B}|^2} \quad (9)$$

The resistivity η has contributions both from electron-ion and electron-neutral collisions. For simplicity, however, in the present treatment we consider η to be the transverse Spitzer resistivity of the plasma.

For the dust flow which is in the $x-z$ plane, the dust vorticity $\boldsymbol{\omega} = \nabla \times \mathbf{U}$ is directed purely along $\hat{\mathbf{y}}$. In small Reynolds number $Re = \frac{LU}{\mu}$ limit for the dust fluid, as described in Ref. [23], nonlinear convective terms are negligible as compared to diffusive terms and under this condition Eqs. (1) and (2) combine to produce the equilibrium equation for $\boldsymbol{\omega}$,

$$\mu \nabla^2 \boldsymbol{\omega} - \nu \boldsymbol{\omega} + \frac{qd}{m_d} (\nabla \times \mathbf{E}_a)_y = 0. \quad (10)$$

From the Eq. (9), we have;

$$\nabla \times \mathbf{E}_a = \eta n_e q_e \left(\nabla \times \frac{\mathbf{E} \times \mathbf{B}}{|\mathbf{B}|^2} \right). \quad (11)$$

Using the standard vector identity for the curl of a vector cross product, we write,

$$\begin{aligned} \nabla \times \frac{\mathbf{E} \times \mathbf{B}}{|\mathbf{B}|^2} = & \mathbf{E} \left(\nabla \cdot \frac{\mathbf{B}}{|\mathbf{B}|^2} \right) - \frac{\mathbf{B}}{|\mathbf{B}|^2} \nabla \cdot \mathbf{E} + \left(\frac{\mathbf{B}}{|\mathbf{B}|^2} \cdot \nabla \right) \mathbf{E} \\ & - (\mathbf{E} \cdot \nabla) \frac{\mathbf{B}}{|\mathbf{B}|^2}. \end{aligned} \quad (12)$$

We note that the first, second and third term of right hand side of Eq. (12) either vanish or negligible for our setup. Specifically, the first term vanishes because magnetic field is divergence-free, $\nabla \cdot \mathbf{B} = 0$, and varies only along z , while the second term approaches zero because sheath electric field E_s is assumed slowly varying in comparison to variation in B in the dust domain. The third term vanishes because there is no gradient in \mathbf{E} along \mathbf{B} either. Under these conditions, Eq. (12) reduces to,

$$\nabla \times \frac{\mathbf{E} \times \mathbf{B}}{|\mathbf{B}|^2} = -(\mathbf{E} \cdot \nabla) \frac{\mathbf{B}}{|\mathbf{B}|^2}. \quad (13)$$

Using the linearized variation of the magnetic field $\mathbf{B}(z) = B_0(1 + \alpha z)$, and the sheath electric field as $\mathbf{E} = E_s \hat{\mathbf{z}}$, the right hand side of the Eq. (13) becomes,

$$\nabla \times \frac{\mathbf{E} \times \mathbf{B}}{|\mathbf{B}|^2} = -E_s \frac{\partial}{\partial z} \frac{1}{B_0(1 + \alpha z)} \hat{\mathbf{y}}. \quad (14)$$

By using Eq. (14) in Eq. (11) we finally obtain $\nabla \times \mathbf{E}_a$ as,

$$\nabla \times \mathbf{E}_a = -\eta n_e q_e E_s \frac{\partial}{\partial z} \frac{1}{B_0(1 + \alpha z)} \hat{\mathbf{y}}, \quad (15)$$

so that the Eq. (10) can be written as,

$$\mu \nabla^2 \boldsymbol{\omega} - \nu \boldsymbol{\omega} + \kappa \boldsymbol{\omega}_a = 0, \quad (16)$$

where the coefficient kappa κ and quantity $\boldsymbol{\omega}_a$ are respectively given as,

$$\kappa = \frac{\eta n_e q_d q_e}{m_d}, \quad (17)$$

and,

$$\boldsymbol{\omega}_a = \boldsymbol{\omega}_{a0} \frac{1}{(1 + \alpha z)^2} = \frac{E_s}{B_0} \frac{\boldsymbol{\alpha}}{(1 + \alpha z)^2}. \quad (18)$$

Here $\boldsymbol{\omega}_a$ is the strength of the vorticity source provided by \mathbf{E} and the magnetic field varying along z ,

The continuity equation for the incompressible dust fluid (3) allows one to define the streamfunction Ψ such that $\mathbf{U} = \nabla \times (\Psi \hat{\mathbf{y}})$ prescribing its the relationship with $\boldsymbol{\omega}$ as,

$$\boldsymbol{\omega} = - \left(\frac{\partial^2 \Psi}{\partial z^2} + \frac{\partial^2 \Psi}{\partial x^2} \right) \hat{\mathbf{y}} \quad (19)$$

The quantity $\boldsymbol{\omega}_a$ replaces the vorticity produced by a non-conservative drive, for example, by the ion drag force in Ref. [23]. Note that a pure electrostatic field produced by sheath structure would still have a zero vorticity and therefore can not act as a source for the dust vortex flow. Remarkably, for a finite number of terms to survive in Eq. (12) it is required that a magnetic field be present essentially. In case of a nonuniform magnetic field and uniform electric field, the first and fourth term can survive. For a magnetic field varying only along z however (as in the present case) the first term vanishes but the fourth term still provides finite contribution. A few more interesting cases would be as follows. In the case of uniform magnetic field, on the other hand, a finite contribution is still possible from second and third terms if a gradient in the electric field is present. If the gradient in the electric field is orthogonal to the direction of B the third term vanishes but the second term can still be finite. In the present setup, as described above, the magnetic field gradient is assumed to be present along a nearly uniform electric field and therefore only the fourth term provides a finite contribution, for the simplicity of the analysis.

Eq. (16) is a fourth order partial differential equation in stream-function and can be solved under the assumptions made in Ref. [23], namely, that the variation of Ψ is determined by the independent choice of driver scale variation along the two orthogonal directions. The confinement domain can therefore be elongated such that the shear effect are stronger only along one of its dimensions. Considering the dependence along x of Ψ , in comparison to that along z , to be produced by the variation the E_a , and that along z to be independently prescribed by variation of B , we choose $L_x \gg L_z$

and the dependence on z and x can be treated via a separable function for Ψ . This allows Ψ to be expressed in the form of the product $\Psi = \Psi_x(x) \Psi_z(z)$ and the equation becomes

$$\left(\frac{\partial^4 \Psi_z}{\partial z^4} + 2k_x^2 \frac{\partial^2 \Psi_z}{\partial z^2} - K_1 \frac{\partial^2 \Psi_z}{\partial z^2} + \Psi_z \frac{\partial^4}{\partial x^4} - K_1 \Psi_z \frac{\partial^2}{\partial x^2} \right) \Psi_x - K_2 \omega_a = 0 \quad (20)$$

having two parameters, $K_1 = \frac{\nu}{\mu}$ and $K_2 = \frac{\kappa}{\mu}$. The procedure for the solution of Eq. 20 is described in the Sec. III.

III. BOUNDARY VALUE PROBLEM IN CARTESIAN SETUP

Eq. (20) is treated as an eigenvalue equation for Ψ_z which is nonzero (bounded) in the region $0 < z/L_z < 1$. However, since the in-homogeneity is introduced by the driver term $K_2 \omega_a$ which remains independent of the boundaries imposed on the dust fluid, a numerical solution with sufficient number of eigenmodes is considered as treated below.

We represent both, the driven dust stream-function and the driver field in term of linear combinations of common eigen functions satisfying the boundary condition imposed on Ψ_z and write, $\Psi_z = \sum_{m=1}^{\infty} c_m \phi_m$ and $\omega_a = \omega_{xa} \sum_{m=1}^{\infty} b_m \phi_m$ [23] with, $\phi_m = \sin(k_m z)$, where $k_m = \frac{\pi m}{L_z}$. The Eq. (20) thus takes the form,

$$\left(F \sum_{m=1}^{\infty} c_m \phi_m \right) \Psi_x = \left(K_2 \sum_{m=1}^{\infty} b_m \phi_m \right) \omega_{xa} \quad (21)$$

Where F represents the operator,

$$F = \frac{\partial^4}{\partial z^4} + 2k_x^2 \frac{\partial^2}{\partial z^2} - K_1 \frac{\partial^2}{\partial z^2} + \frac{\partial^4}{\partial x^4} - K_1 \frac{\partial^2}{\partial x^2} \quad (22)$$

In order to reduce Eq. (21) to a solvable eigenvalue problem under certain special conditions, we now consider the case where along the direction of weak variation, x , the dust is driven as a single eigenmode $\Psi_x = c_x \phi_x$, by a corresponding single eigenmode of the driver $\omega_{xa} = b_x \phi_x$. This readily allows us to redefine the known and unknown coefficients b_m and c_m , respectively, as $b_m \rightarrow b_x b_m$ and $c_m \rightarrow c_x c_m$, and the Eq. (21) reduces into a solvable form,

$$F \sum_{m=1}^{\infty} c_m \phi_m = K_2 \sum_{m=1}^{\infty} b_m \phi_m. \quad (23)$$

The eigenvalue equation for the operator F can be written as,

$$(F - \lambda_m) \sin(k_m z) = 0, \quad (24)$$

where the eigenvalues λ_m are,

$$\lambda_m = k_m^4 + K_1 k_m^2 - (2k_m^2 + K_1) k_x^2 + k_x^4. \quad (25)$$

The unknown coefficients c_m need to be obtained from the solution of a set of M simultaneous equations to be given from

the relation,

$$\sum_{m=1}^M (\lambda_m c_m - K_2 b_m) \sin(k_m z) = 0, \quad (26)$$

where M represents the limiting value of the number of modes sufficient to reproduce the smallest length scale in the problem. When rewritten in terms of unknown coefficients c_m of the problem which need to be determined, (26) takes a more familiar form,

$$A_{im} c_m = B_i, \quad (27)$$

where A_{ij} is the matrix of the coefficients, with i being the index for the spatial locations z_i where solutions values ($\Psi_z(z_i)$ values) are desired. These coefficients and the vector B_i in this new form become,

$$A_{im} = \lambda_m \sin(k_m z_i) \quad (28)$$

$$\text{and } B_i = K_2 \sum_{j=1}^M b_j \sin(k_j z_i) \quad (29)$$

Since the elements of \mathbf{A} and \mathbf{B} are known, the solution for the streamfunction involves determining the values of coefficients c_m using the inversion,

$$c_m = \mathbf{A}^{-1} \mathbf{B} \quad (30)$$

The boundary conditions on $U_x = -\frac{\partial \Psi_z}{\partial z}$ can further be imposed requiring the z profile of streamfunction to have a desired derivative. This procedure is adopted for the solutions presented in the Sec. IV where effect of magnetization of electrons are investigated on the dust vortex flow dynamics.

IV. DUST VORTEX FLOW SOLUTIONS IN A NON-UNIFORM MAGNETIC FIELD

In the following analysis, the values of quantities (mass, length, velocity etc.) associated with a typical dusty plasma set up are used to scale the parameters and variables involved in the above analytic formulation. We accordingly use dust mass m_d , ion acoustic velocity U_A , dust charge q_d and length of the simulation box L_z values in a typical dusty plasma to normalize our variables such that, the variables ω , κ and ν have the unit $\frac{U_A}{L_z}$, the variables Ψ and μ have the unit $U_A L_z$ and the variables E_s , η and B_0 have the units $\frac{m_d U_A^2}{q_d L_z}$, $\frac{m_d U_A L_z^2}{q_d^2}$, and $\frac{m_d U_A}{q_d L_z}$, respectively.

For parameters corresponding to a typical weakly magnetized dusty plasma [21] where $m_d = 1 \times 10^{-14}$ Kg, $L_z = 0.1$ m, $U_A = 2.5 \times 10^3$ m/sec, charge on the dust $q_d = 1.6 \times 10^{-16}$ C [24], electric field 10^3 Vm $^{-1}$ and magnetic field 10-100 G, we estimate the typical values of our input parameters as the electric field $E_s = 2.5 \times 10^{-7} \frac{m_d U_A^2}{q_d L_z}$, the magnetic field $B_0 = 6.4 \times 10^{-10} \frac{m_d U_A}{q_d L_z}$, and $\alpha = 1 \frac{L_z^{-1}}$ which provide, $\omega_{a0} = 4 \times 10^2 U_A / L_z$, $\eta = 10^{-20} \frac{m_d U_A L_z^2}{q_d^2}$ [25], $n_e = 10^{13} L_z^{-3}$, and $\kappa = 10^{-10} \frac{U_A}{L_z}$.

Note that a rather stronger resistivity because of the electron-neutral (e-n) collisions would be more appropriate for high pressure cases experimentally analyzed by Puttscher and Melzer [21] where the $\eta \equiv \eta_{en}$ value should be a few order higher than the standard Spitzer resistivity mentioned above. Considering that the E_a value produced rather by electron-neutral resistivity ($\sim \eta_{en} n_e \frac{E_s}{B_0}$) still remains sufficiently lower than the lowest order electric field (or above E_s value), as required for the analysis to hold good, larger values of η remain equally admissible. We however use the above representative Spitzer resistivity value for all our computations presented here. For the present numerical solutions we have used large number of eigenmodes ($M=200$) to express the resulting dust stream-function Ψ_z at equal number of locations z_i .

The solutions in the present treatment are obtained in the rectangular domain measuring L_z along z and $20L_z$ along x directions as appropriate for the limit $k_x \ll k_z$ of the analysis. The profile for the source field ω_a given by Eq. (18) considered for this analysis, using $B_0 = 6.4 \times 10^{-10} \frac{m_d U_A}{q_d L_z}$ and $\alpha = 1 L_z^{-1}$, is presented in Fig.2(a) as generated by a linear variation in the applied magnetic field that remains independent of the dust boundaries. The choice of applying boundary condition for the dust flow is available only at $z = 0$ and $z = L_z$ which correspond to two adjacent sides of the rectangular dust confinement domain in the x - z plane. We have applied dissimilar boundary conditions for the dust flow velocity along these two boundaries. For example, a no-slip boundary condition is applied at the lower boundary, $z = L_z$ while no control on the velocity values is done on the boundary at $z = 0$ where the dust velocity is freely determined by the driver strength.

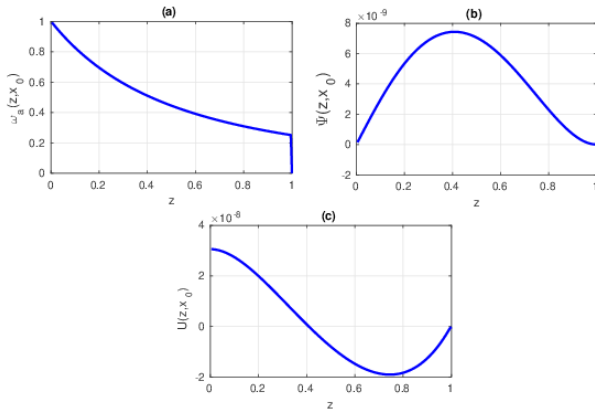


Figure 2: Functions for dust flow profile plotted at $x = x_0 = L_x/2$. (a) driver profile, $\omega_a = 4 \times 10^2$, (b) dust stream-function, $\Psi(z, x_0)$, and (c) x-component of dust velocity profile for $\mu = 0.01 U_A L_z$, $\nu = 0.1 \frac{U_A}{L_z}$, $B_0 = 6.4 \times 10^{-10} \frac{m_d U_A}{q_d L_z}$, $\alpha = 1 L_z^{-1}$ and $\kappa = 10^{-10} \frac{U_A}{L_z}$.

A range for value of dust viscosity $\mu = 0.01$ to $0.001 U_A L_z$, is chosen considering the dust fluid flow to be in small Reynolds number limit (≤ 1) as given in Sec. II which is consistent with the present linear limit considered of the model.

The collision frequency $\nu = 0.1 U_A/L_z$ is considered here for sufficient high pressure regime, for example that described by Puttscher and Melzer [21] where ambipolar field effects dominates the ion drag force.

The profile for dust streamfunction Ψ at $x = L_x/2$ is presented in Fig. 2(b) driven by source field ω_a which is provided by the combination of sheath electric field and non-uniform applied magnetic field. The boundary conditions on dust streamfunction discussed above ensures zero dust velocity at $z = L_z$, as plotted in Fig.2(c), and is independent of the driver strength at this boundary. A zero net flux of dust particles crosses the $x = L_x/2$ line as indicated by the velocity profile presented in Fig.2(c) which has equal area under the positive and negative region of the curve considering that the dust fluid is incompressible.

The ambient electric field along z ($0,0,E$) and the applied weak magnetic field along y ($0,B,0$) cause only the electrons to drift in negative x -direction as the ions are unmagnetized. The displacement of electrons generates a space-charge field which is directed along negative x direction. The negatively charged dust must flow along positive x because of this electric field and it experiences a force ($\mathbf{F}_E = -q_d \mathbf{E}_a$). However since the magnetic field has a gradient along z , the electron drift is nonuniform in z and the space charge field \mathbf{E}_a generated by the electrons displacement is nonuniform along z . As a result, the dust velocity profile has a change of sign in the region as the dust experiences a larger force in positive x direction at small z values and must flow in along this force. Due to its incompressible character, however, a return flow is set up through the region of large z where the ambipolar field \mathbf{E}_a is weaker and therefore the dust velocity sign is opposite, setting up vortex flow.

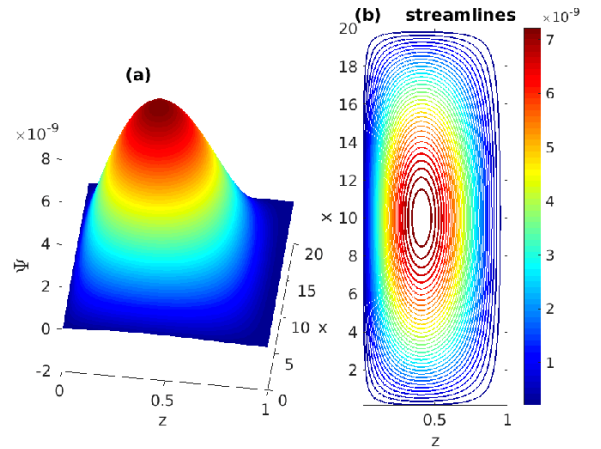


Figure 3: 2D-functions for dust flow profiles, (a) dust stream function $\Psi(z, x)$, and (b) dust streamlines.

The sign of the dust flow in the region of strong ambipolar field in our case is consistent to the Melzer and Puttscher [22] where they have observed the displacement of the dust particles in negative $\mathbf{E} \times \mathbf{B}$ direction at sufficiently high gas pressure.

The 2D surface plot of the streamfunction solution is pre-

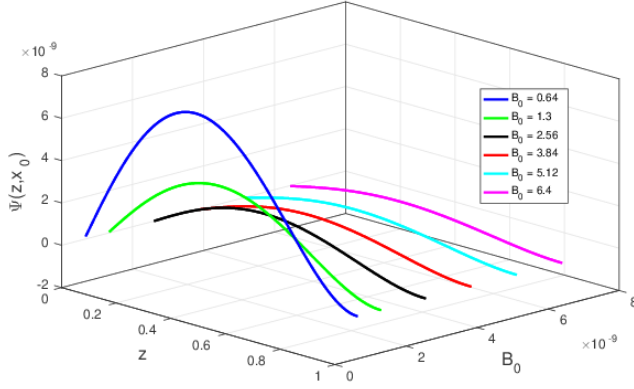


Figure 4: Dust stream-function profiles with different values of magnetic field B_0 and $\alpha = 1$.

sented in Fig.3(a) for the case using $\mu = 0.01 U_A L_z$, $\nu = 0.1 \frac{U_A}{L_z}$, $\alpha = 1 L_z^{-1}$, $\kappa = 10^{-10} \frac{U_A}{L_z}$, which obeys the applied boundary conditions at the boundaries at $z = 0$ and $z = L_z$, respectively. Similarly, the confinement of dust fluid in x-direction is ensured by uniformity in the value of Ψ along z at boundaries $x = 0, L_x$, such that $\partial\Psi/\partial z = 0$ at these boundaries and the dust fluid remains confined in region $0 < x < L_x$. The topology of the surface plot corresponds to a vortex structure in dust velocity field and the corresponding streamlines of dust flow is presented in Fig.3(b). This shows that the ambipolar electric field can act as a source of finite vorticity in the dust flow dynamics. Although the ambient time independent electric and magnetic fields included here provide only conservative forcing mechanisms, when a drift based mechanism is considered the dust vortex flow solutions are recovered. The dust streamlines in Fig. 3(b) is clear evidence of dust vortex formation. The emergence of macroscopic dust vortex flow becomes possible by non-zero value of parameter α responsible for the simplest non-uniformity introduced by α .

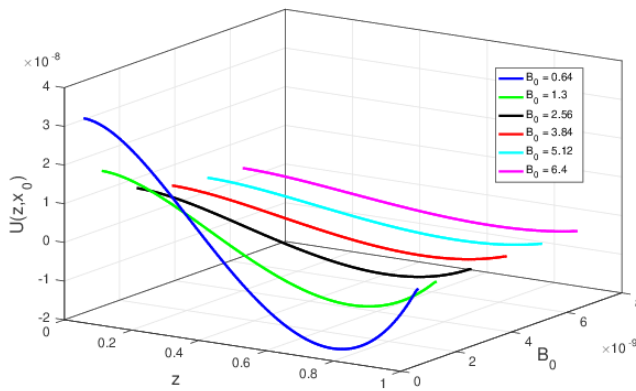


Figure 5: x-component of dust velocity profiles with different values of magnetic field B_0 and $\alpha = 1$.

The dust streamfunction profiles plotted at $x = L_x/2$ with the variation of magnetic field strength B_0 is presented in Fig. 4, for the parameters $\mu = 0.01 U_A L_z$, $\nu = 0.1 \frac{U_A}{L_z}$, $\alpha = 1 L_z^{-1}$, $\kappa = 10^{-10} \frac{U_A}{L_z}$. Dust gradient of streamfunction gradually reduces to a minimum value with increase in applied magnetic field strength B_0 . Therefore, as from the Eq. (19), vorticity associated with circulation motion of dust flow field also tends to reduced with strength of applied magnetic field B_0 . The corresponding dust velocity flow field profiles are presented in Fig.5 showing that the magnitude of the maximum dust velocity achieved at $z = 0$ decreases with increase in applied magnetic field strength B_0 . In present analysis the dust velocity is determined by the combination of ambipolar electric field, \mathbf{E}_a , neutral drag, ν and kinematic viscosity, μ , of dust fluid. For the fixed values of ν and μ , however, the dust velocity is determined only by ambipolar force as presented in Fig.5. Since the ambipolar electric field \mathbf{E}_a has a inverse relation with magnetic field as given by Eq.(9), the electrostatic force ($\mathbf{F}_E = -q_d \mathbf{E}_a$) arising from the ambipolar field reduces with the magnetic field. As a result, the dust vortex flow weakens at higher magnetic field as shown in Fig.5. The effect of \mathbf{B} field strength analyzed on the ambipolar field here is therefore in contrast to the effect of \mathbf{E} field strength that may be present in the plasma sheath and would instead strengthen the vortex flow.

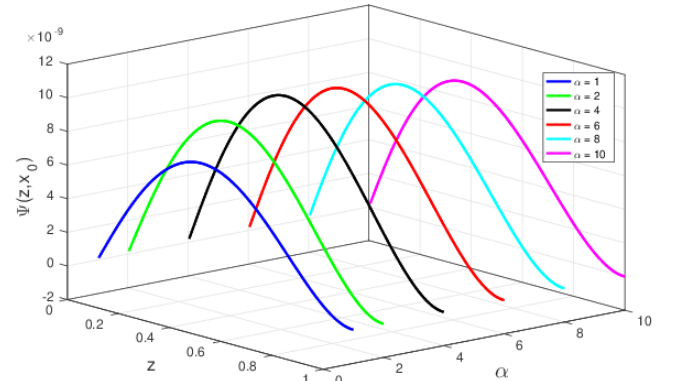


Figure 6: Dust stream-function profiles with different values of α and constant magnetic field $B_0 = 6.4 \times 10^{-10}$.

Analysis of dust flow field with varying applied magnetic field gradient α is presented in Figs.6 and 7. Dust stream-function peak value first increases and then slightly decreases with increasing α as shown in Fig.6 at constant magnetic field strength $B_0(z = 0) = 6.4 \times 10^{-10} \frac{m_d U_A}{q_d L_z}$. The corresponding dust velocity field profiles are presented in Fig.7. Peak dust velocity (at $z = 0$) similarly shows a maximum with respect to α however its variation remains comparatively weaker at larger values of α .

Effect of kinematic viscosity μ on dust velocity in non-uniform magnetic field has been analyzed in Fig.8 with magnetic field strength $B_0(z = 0) = 6.4 \times 10^{-10} \frac{m_d U_A}{q_d L_z}$ and $\alpha = 1 L_z^{-1}$. With the application of the no-slip boundary condition

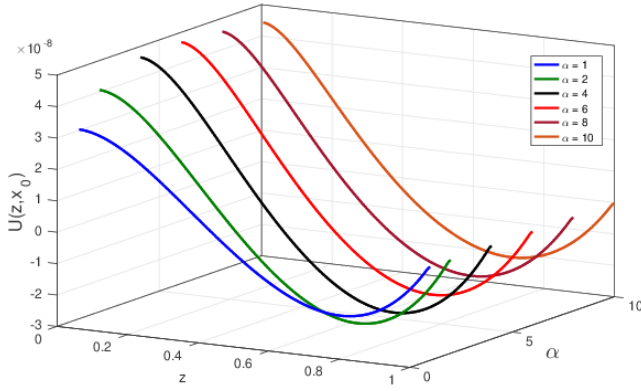


Figure 7: x-component of dust velocity profiles with different values of α and constant magnetic field

$$B_0 = 6.4 \times 10^{-10}.$$

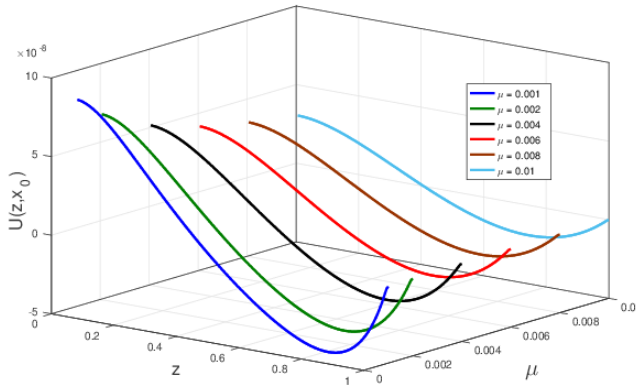


Figure 8: x-component of dust velocity profiles with different values of viscosity of dust fluid

$$\mu, \text{ for } \alpha = 1 \text{ and } B_0 = 6.4 \times 10^{-10}.$$

at the boundary $z = L_z$ we note in Figs. 5 and 7 a negligible effect of magnetic field strength and its gradient, respectively, on the width of the boundary layer that forms and must shrink with reducing μ [23] as presented in Fig. 8 for the present case. The vortex flow is also seen to weaken with increasing μ .

V. DUST VORTEX SOLUTIONS FOR MULTIPOLAR FORM OF THE AMBIPOLAR FIELD

We finally explore the cases where the modulation in magnetic field strength can result in multipolar structure of the ambipolar electric field \mathbf{E}_a . This effect is achieved by examining cases with individual modes in the magnetic field gradient driving the vortex flow and using increasing values $m = 1, 2$ and 3 of the mode number m while using the strength of this effect as determined by the factor κ . Note that the quantity ω_a

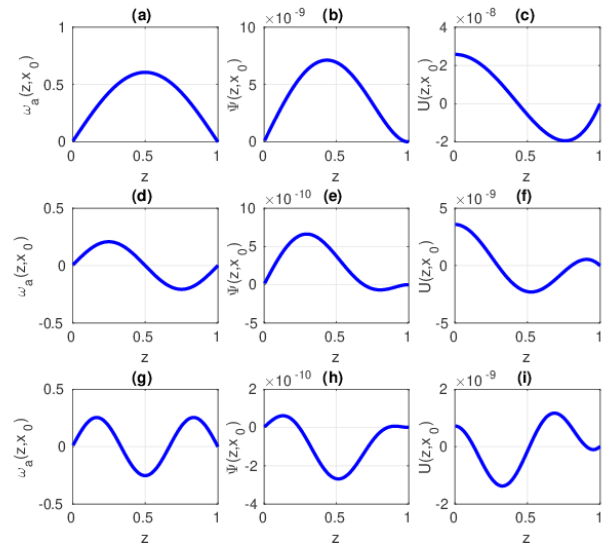


Figure 9: Functions for the dust flow profiles with different driver mode number (a) driver profile ω_a (b) dust stream function $\Psi(z, x_0)$ and (c) x-component of dust velocity profile for mode ($m=1$) and similarly fig. (d),(e),(f) and (g),(h),(i) for $m = 2$ and $m=3$, respectively, for $\alpha = 1$ and $B_0 = 6.4 \times 10^{-10}$.

is an effective source of vorticity produced by the shear in the ambipolar electric field present in Eq. (20) and arising, in this case, from a rather *wave-like* spatial variation of the ambient magnetic field.

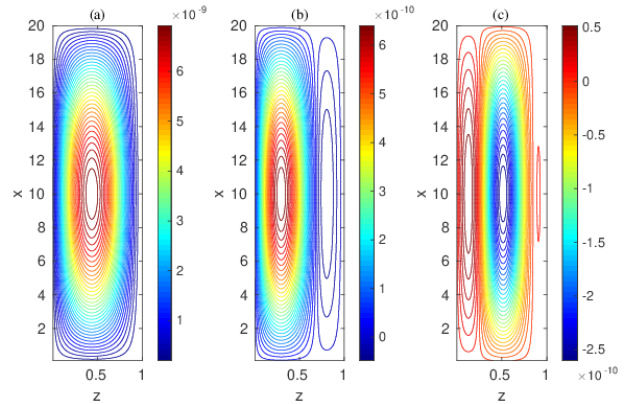


Figure 10: streamlines for the dust fluid flow, with different driver mode number (a) $m=1$ (b) $m=2$ (c) $m=3$ using parameters $\alpha = 1$ and $B_0 = 6.4 \times 10^{-10}$.

As presented in Fig.9, the source field having an individual mode number $m = 1$ in Fig.9(a) produces a single peak profile of the streamfunction plotted in Fig.9(b) and the corresponding dust velocity plotted in Fig.9(c) has a single dust vortex. The streamlines corresponding to this case are plotted in Fig.10(a) showing a single 2D vortex flow structure. For the case $m = 2$ as presented in Fig.9(d)-(f), however, a velocity

profile consistent with a set of two counter-rotating vortices emerges. The corresponding dust streamlines in Fig.10(b) clearly show this set of counter-rotating vortex flow structures. A further increase in the m value, $m = 3$, similarly produces a sequence of three counter-rotating dust vortex flow structures as presented in Fig.9(g)-(i) and Fig.10(a). The third vortex close to the boundary $z = L_z$ in this case however has a very low strength because of the flow satisfying a no-slip boundary condition at this boundary.

VI. SUMMARY AND CONCLUSIONS

To summarize, we have presented an analysis of a dust vortex flow in the electrically charged dust medium suspended in a weakly magnetized plasma. We have examined the cases where a sheared $\mathbf{E} \times \mathbf{B}$ drift, arising from a spatially non-uniform magnetic field, is able to drive a vortex motion of the suspended dust fluid. By employing the $\mathbf{E} \times \mathbf{B}$ effect on dust particles as recovered and described by Melzer and Puttscher [22], we have shown that the ambipolar electric field can act as a source of finite vorticity in the dust flow dynamics. The expressions derived by us use the circulation of the ambipolar field generated by $\mathbf{E} \times \mathbf{B}$ drift of the electrons as a driver for vortex flow of the dust motion allowing study of its behavior in presence of nonuniform magnetic field. The results characterize nature of dependence of the dust vortex motion on the

strength of magnetic field and its gradient.

The dust streamfunction solutions in a Cartesian setup obtained under applied non-uniform magnetic field $B(z)$ and its linear gradient α , over the dust confinement domain, show that a combination of conservative fields (magnetic and electric field) can generate a finite circulation in dust flow field. The resulting dust vortex flow driven is therefore driven in the absence of any non-conservative fields, e.g., friction, ion drag and the dust charge variation. A multipolar nature of the ambipolar electric field is additionally recovered for wave-like nature of the spatial gradients and is examined in terms of a sequence of counter-circulating dust vortex flow produced by it for larger mode number of the magnetic field variation. The vortex flow motion of the highly charged dust medium in a magnetized plasma environment, arising purely from the field non-uniformity can be an interesting effect for magnetized dusty plasma, both laboratory experiments and in natural conditions, such as in astrophysical circumstances. The present first study of this process can thus provide quantitative inputs for conducting the related laboratory experiments for exploring the deeper correlation between the two.

VII. AIP PUBLISHING DATA SHARING POLICY

The data that support the findings of this study are available from the corresponding author upon reasonable request.

-
- [1] Y. Saitou and O. Ishihara, *Physical review letters* **111**, 185003 (2013).
- [2] P. Shukla, *Physics of Plasmas* **8**, 1791 (2001).
- [3] P. Shukla and A. Mamun, *New Journal of Physics* **5**, 17 (2003).
- [4] S. Nunomura, N. Ohno, and S. Takamura, *Japanese journal of applied physics* **36**, 877 (1997).
- [5] F. M. Cheung, N. J. Prior, L. W. Mitchell, A. A. Samarian, and B. W. James, *IEEE transactions on plasma science* **31**, 112 (2003).
- [6] U. Konopka, D. Samsonov, A. Ivlev, J. Goree, V. Steinberg, and G. Morfill, *Physical Review E* **61**, 1890 (2000).
- [7] V. Y. Karasev, E. Dzlieva, A. Y. Ivanov, and A. Eikhvald, *Physical Review E* **74**, 066403 (2006).
- [8] T. Hall, E. Thomas Jr, K. Avinash, R. Merlino, and M. Rosenberg, *Physics of Plasmas* **25**, 103702 (2018).
- [9] E. Thomas, U. Konopka, D. Artis, B. Lynch, S. Leblanc, S. Adams, R. Merlino, and M. Rosenberg, *Journal of Plasma Physics* **81** (2015).
- [10] S. Khrapak, A. Ivlev, G. Morfill, and H. Thomas, *Physical review E* **66**, 046414 (2002).
- [11] S. Khrapak and G. Morfill, *Contributions to Plasma Physics* **49**, 148 (2009).
- [12] M. Kaur, S. Bose, P. Chattopadhyay, D. Sharma, J. Ghosh, and Y. Saxena, *Physics of Plasmas* **22**, 033703 (2015).
- [13] V. Vladimirov, L. Deputatova, A. Nefedov, V. Fortov, V. Rykov, and A. Khudyakov, *Journal of Experimental and Theoretical Physics* **93**, 313 (2001).
- [14] S. Mitic, R. Sütterlin, A. I. H. Höfner, M. Thoma, S. Zhdanov, and G. Morfill, *Physical review letters* **101**, 235001 (2008).
- [15] M. Schwabe, L. Hou, S. Zhdanov, A. Ivlev, H. Thomas, and G. Morfill, *New Journal of Physics* **13**, 083034 (2011).
- [16] D. Law, W. Steel, B. Annaratone, and J. Allen, *Physical review letters* **80**, 4189 (1998).
- [17] G. Uchida, S. Iizuka, T. Kamimura, and N. Sato, *Physics of Plasmas* **16**, 053707 (2009).
- [18] M. Klindworth, A. Melzer, A. Piel, and V. Schweigert, *Physical Review B* **61**, 8404 (2000).
- [19] T. Miksch and A. Melzer, *Physical Review E* **75**, 016404 (2007).
- [20] M. Puttscher and A. Melzer, *New Journal of Physics* **16**, 043026 (2014).
- [21] M. Puttscher and A. Melzer, *Physics of Plasmas* **21**, 123704 (2014).
- [22] A. Melzer and M. Puttscher, *Physics of Plasmas* **24**, 053701 (2017).
- [23] M. Laishram, D. Sharma, and P. K. Kaw, *Physical Review E* **91**, 063110 (2015).
- [24] S. Khrapak, S. V. Ratynskaia, A. Zobnin, A. Usachev, V. Yaroshenko, M. Thoma, M. Kretschmer, H. Höfner, G. Morfill, O. Petrov, *et al.*, *Physical Review E* **72**, 016406 (2005).
- [25] F. Chen, *Introduction to Plasma Physics and Controlled Fusion* (Springer, 2015).